

## Supplemental Material

[Supplemental\\_Fig\\_S1.pdf](#)

[Supplemental\\_Fig\\_S2.pdf](#)

[Supplemental\\_Fig\\_S3.pdf](#)

[Supplemental\\_Fig\\_S4.pdf](#)

[Supplemental\\_Fig\\_S5.pdf](#)

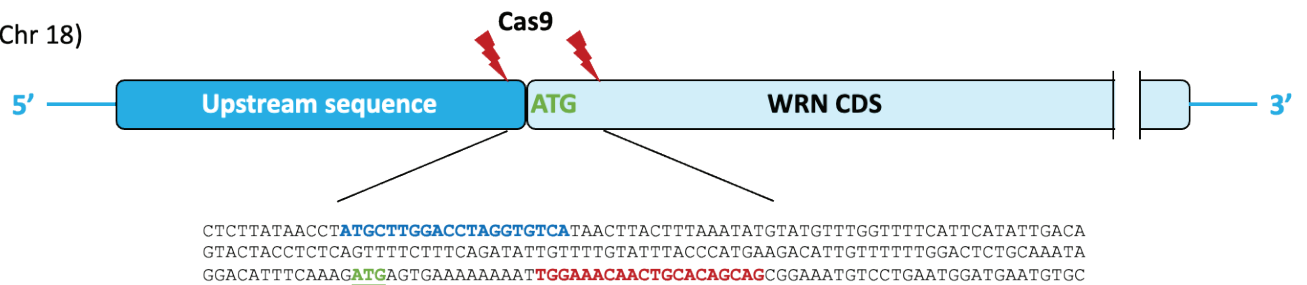
[Supplemental\\_Fig\\_S6.pdf](#)

[Supplemental\\_Fig\\_S7.pdf](#)

[Supplemental\\_Movie\\_S1.avi](#)

[Supplemental\\_Table\\_S1.xlsx](#)

A

*WRN* gene (Chr 18)

B

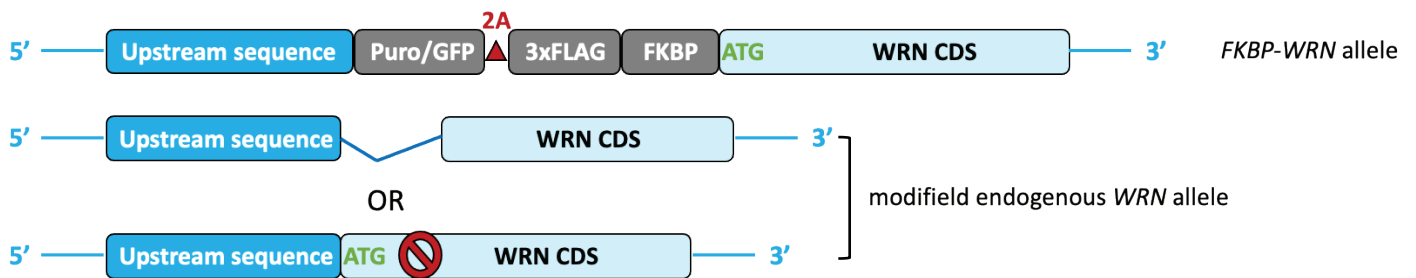
**(i) homozygous knock-in of *FKBP-WRN***

RKO c11, KM12 c2, HCT116 c9

**(ii) heterozygous knock-in of *FKBP-WRN***

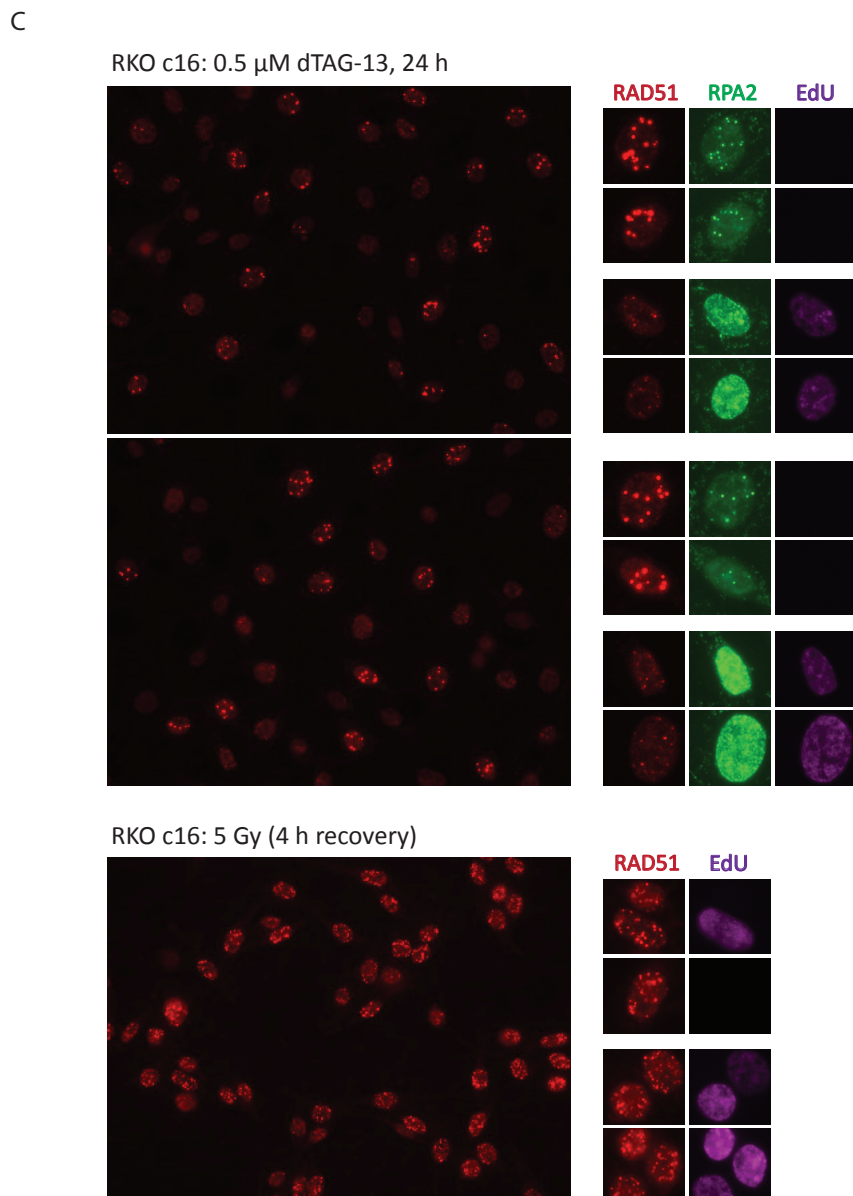
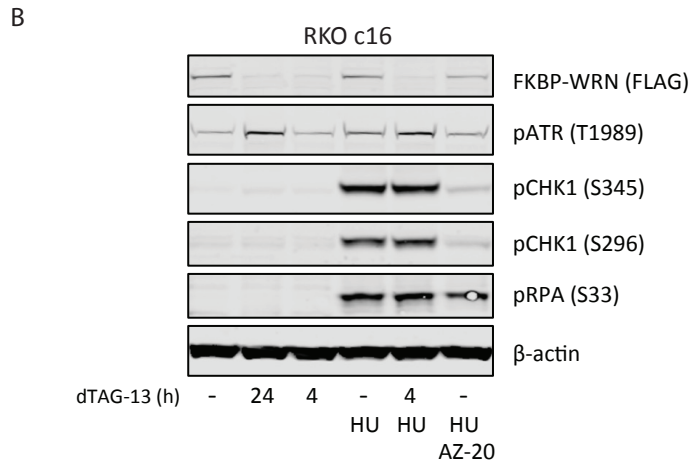
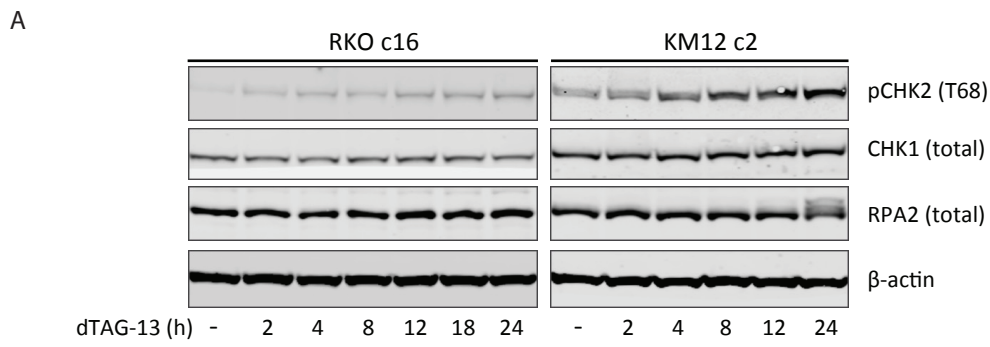
RKO c16, KM12 c5, OVCAR8 c2, OVCAR8 c8

HCT116 c8



**Supplemental Figure S1. Verification of FKBP-WRN knock-in at the endogenous WRN**

**locus.** (A) Schematics depicting the locations of the two sgRNAs (in blue and red) used to target the WRN gene. The translation initiation site of WRN is indicated by the green underlined ATG codon. (B) Confirmation of successful FKBP-WRN knock-in. Genomic DNA was extracted from candidate clones and amplified by PCR prior to Sanger sequencing. Note that both homozygous and heterozygous FKBP-WRN knock-in clones were obtained. In the case of heterozygous knock-in, the remaining allele of WRN was found to be inactivated by small indels that either excised the initiation ATG or produced a STOP codon slightly downstream of the ATG.



**Supplemental Figure S2. Short-term DNA damage responses in MSI-H cancer cells**

**following acute WRN degradation.** (A) RKO and KM12 clones expressing FKBP-WRN were treated or not with 0.5  $\mu$ M dTAG-13 for the indicated amount of time. Immunoblotting showed the levels of pCHK2, CHK1 and RPA2 as a function of time. One of two independent

experiments is shown. (B) RKO c16 was treated or not with 0.5  $\mu$ M dTAG-13 for 4 or 24 h.

Where indicated, 3 mM HU and/or 1  $\mu$ M AZ-20 was added to the growth media for 2 h.

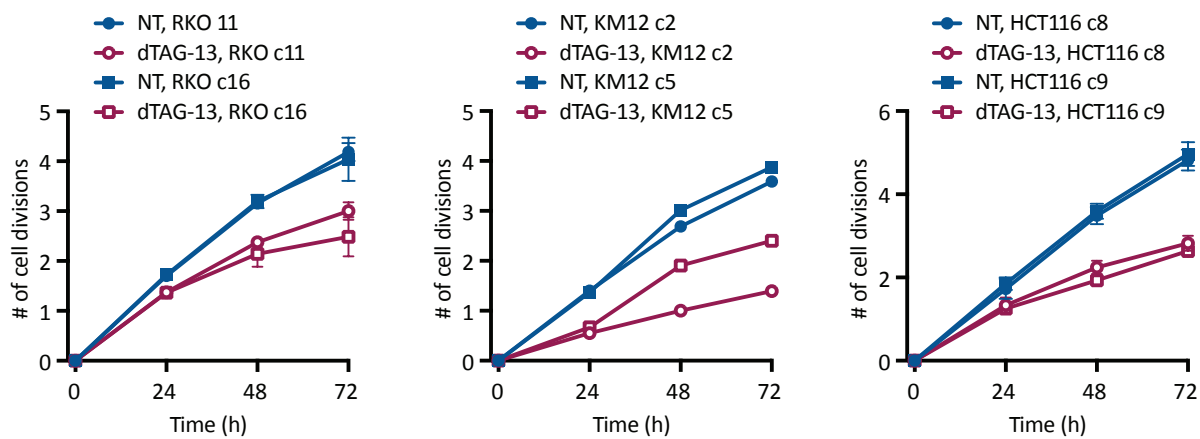
Immunoblotting showed that ATR autophosphorylation, ATR-mediated CHK1 (S345) and RPA (S33) phosphorylation and CHK1 autophosphorylation (S296) were induced by HU regardless of

the WRN status. A representative experiment is shown. (C) RKO c16 was treated or not with 0.5  $\mu$ M dTAG-13 for 24 h or  $\gamma$ -irradiated with 5 Gy and allowed to recover for 4 h.

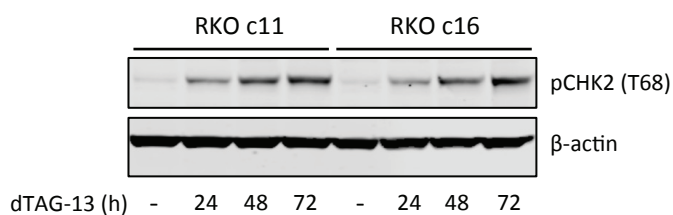
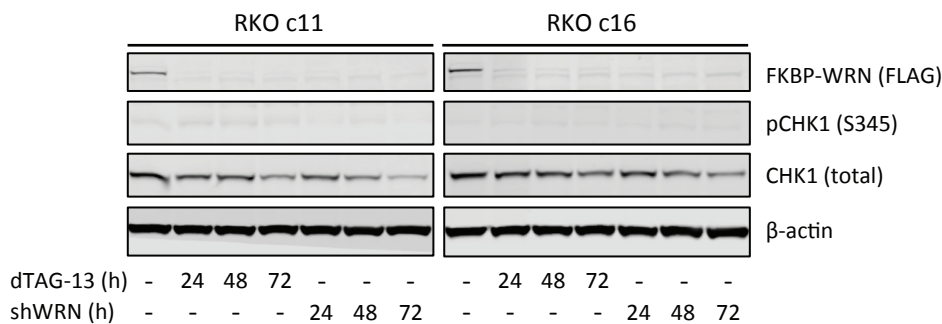
Immunofluorescence staining showed enlarged RAD51 foci in dTAG-treated G2 cells, as

compared to RAD51 foci found in S-phase cells. By contrast, irradiation induced RAD51 foci of comparable sizes in S and G2. One of two independent experiments is shown.

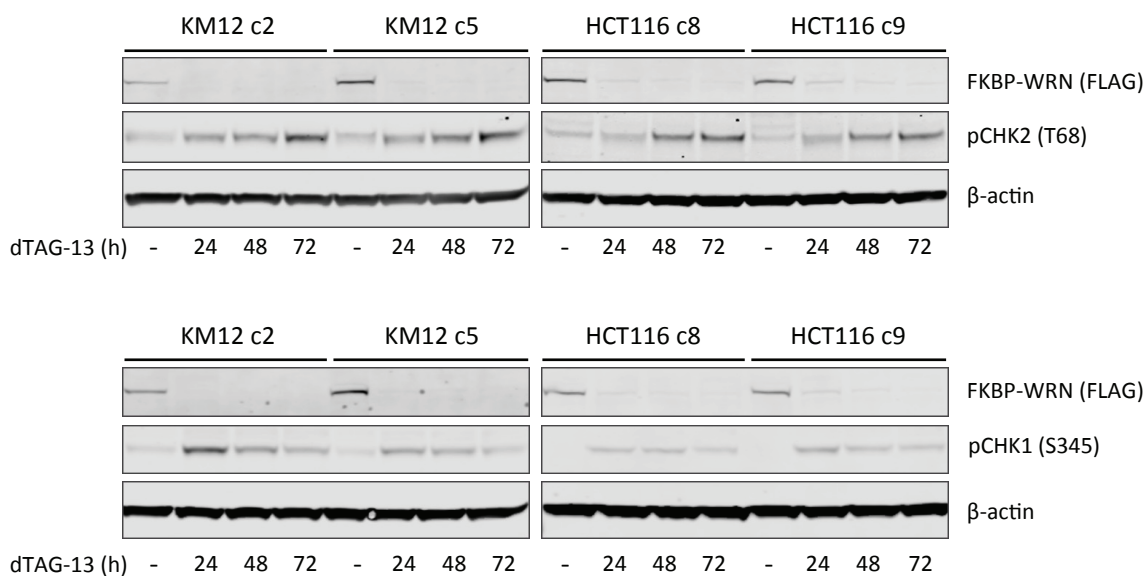
A



B

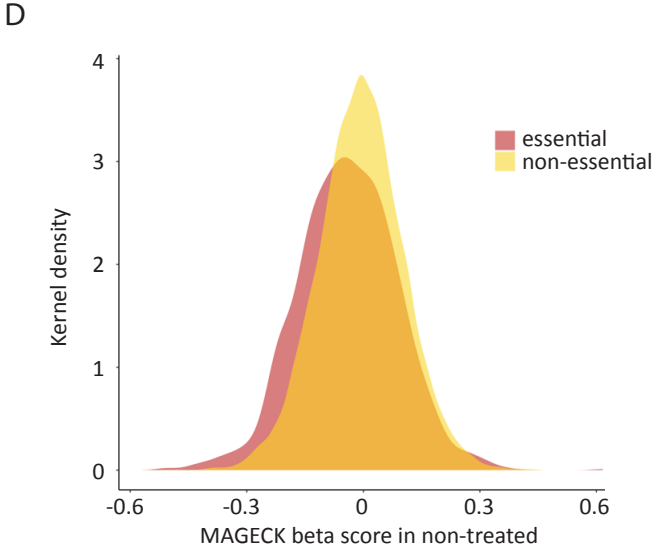
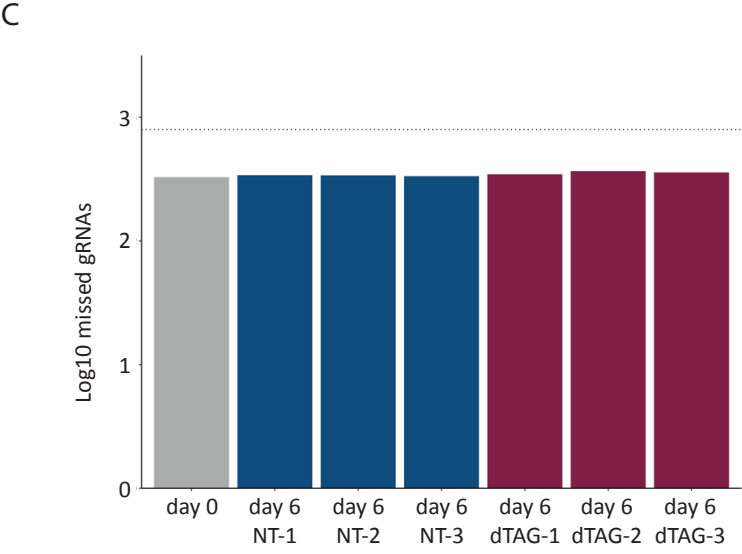
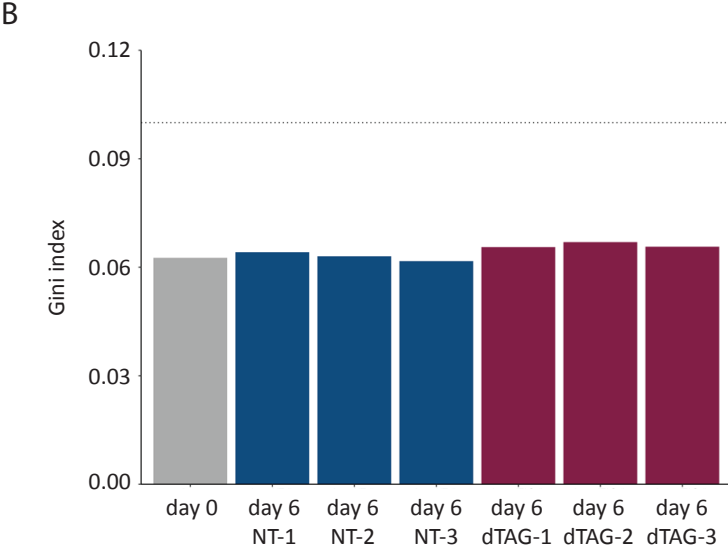
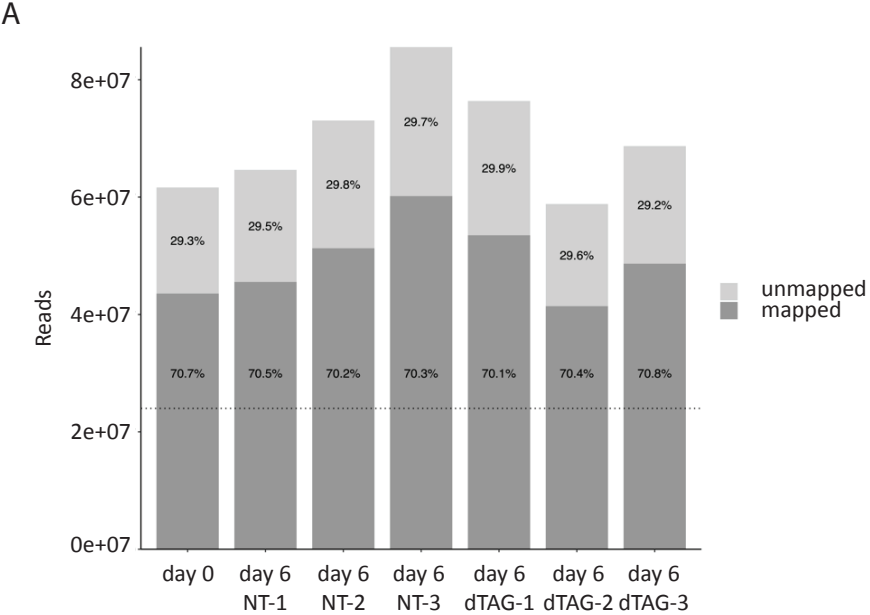


C



**Supplemental Figure S3. Long-term DNA damage responses in MSI-H cancer cells**

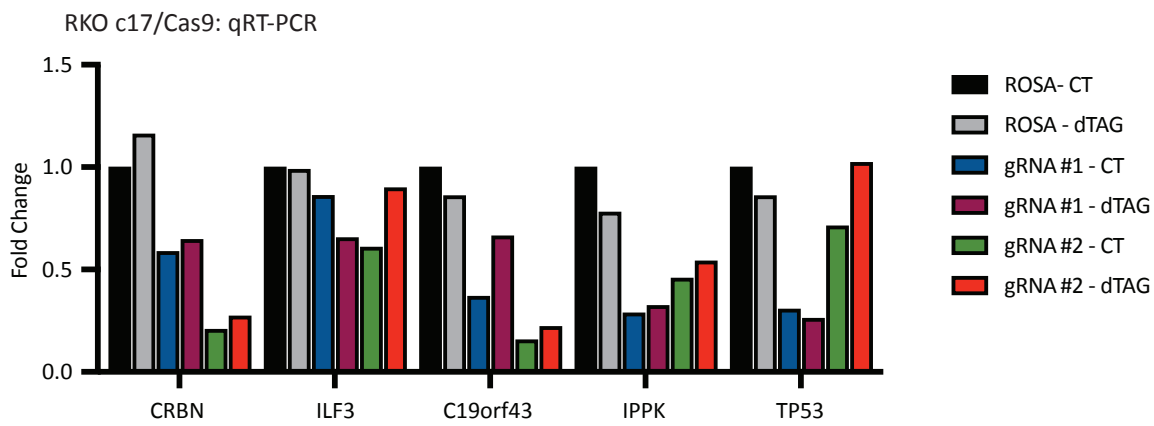
**following acute WRN degradation.** (A) RKO, KM12 and HCT116 clones expressing FKBP-WRN were pre-labeled with 5  $\mu$ M CFSE and then treated or not with 0.5  $\mu$ M dTAG-13. FACS analyses of live cells at the indicated post-treatment times showed that dTAG-treated MSI-H cancer cells could still divide, albeit at a reduced rate compared to vehicle-treated counterparts. Average of three (RKO, HCT116) or two (KM12) independent experiments is shown. (B) RKO clones expressing FKBP-WRN were treated or not with 0.5  $\mu$ M dTAG-13 or with 1  $\mu$ g/mL doxycycline for the indicated amounts of time. Immunoblotting showed progressive induction of CHK2 phosphorylation, but not that of CHK1. Total CHK1 protein level remained unchanged over time. One of two independent experiments is shown. (C) KM12 and HCT116 clones expressing FKBP-WRN were treated or not with 0.5  $\mu$ M dTAG-13 for the indicated amounts of time. Immunoblotting showed progressive induction of pCHK2 over time. Phosphorylation of CHK1 was also induced but did not seem to increase over time.



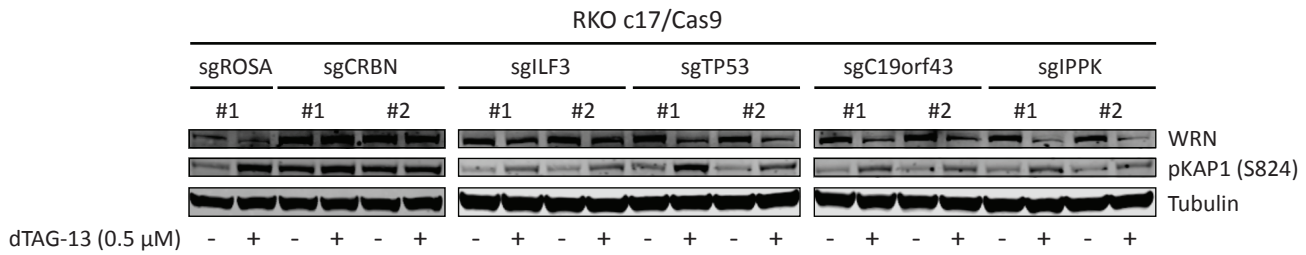


**Supplemental Figure S4. Quality control metrics for CRISPR screen.** (A) Mapped and unmapped reads for each sample. Dotted line represents minimum acceptable mapped reads. (B) Gini index for each sample. Dotted line represents highest acceptable Gini index. (C) Missed gRNAs for each sample. Dotted line represents highest acceptable missed gRNAs for the Brunello library. (D) Change in distribution of beta scores for essential and non-essential genes in the untreated condition. Essential genes were taken from DepMap, Broad (2023) (CRISPRInferredCommonEssentials); dataset: <https://doi.org/10.6084/m9.figshare.22765112.v2>

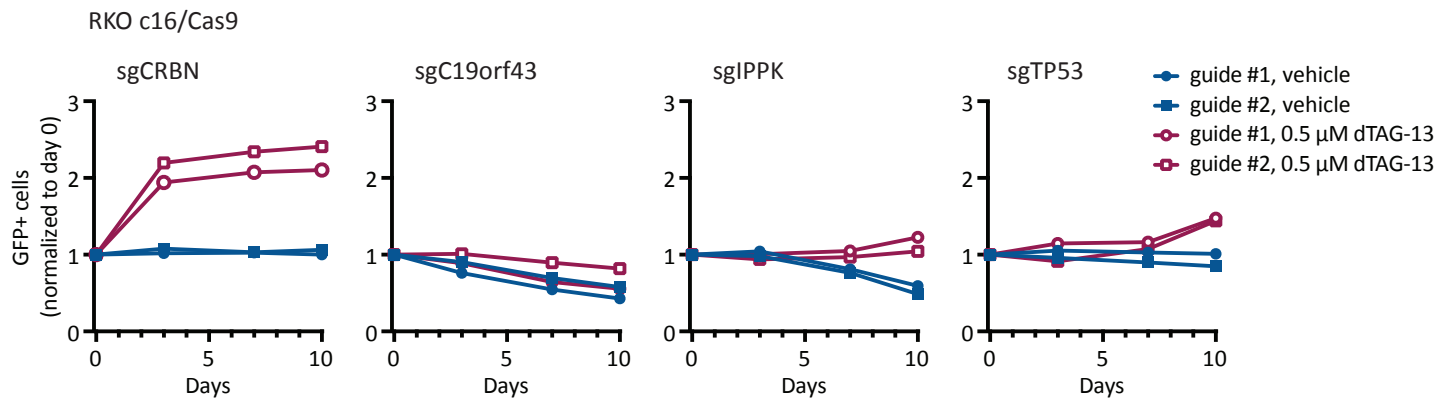
A



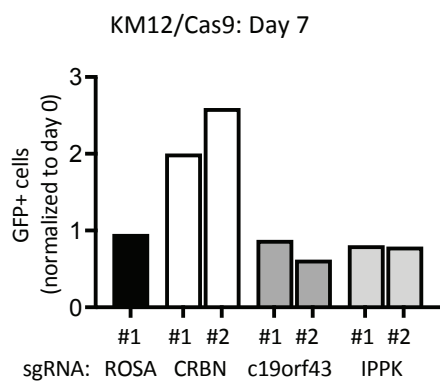
B



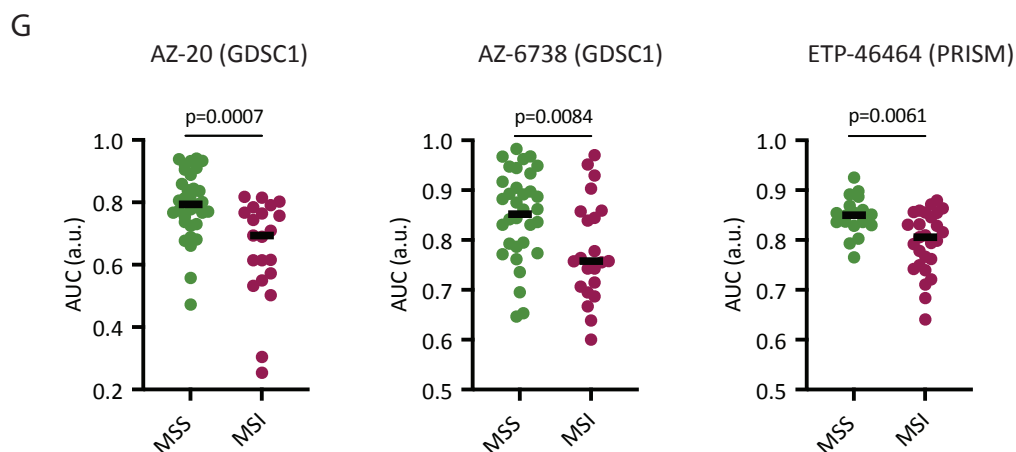
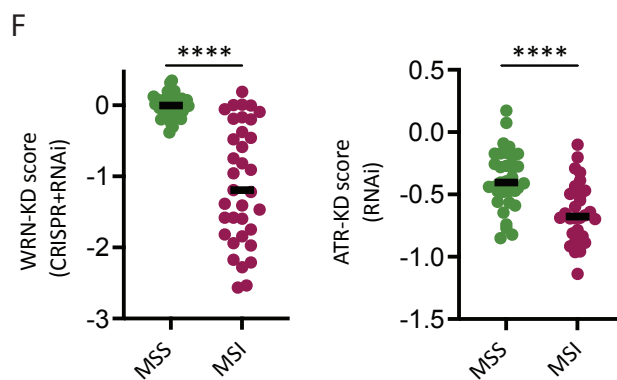
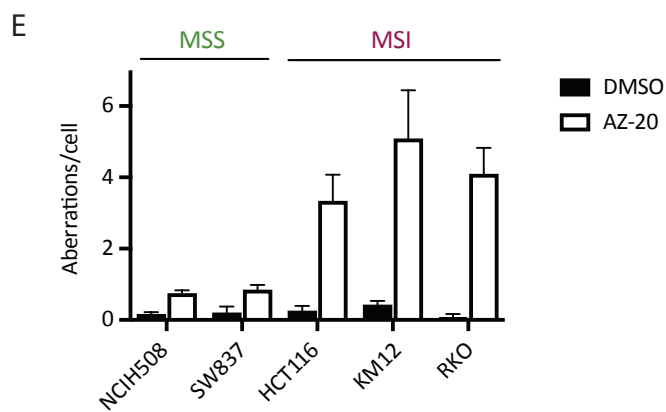
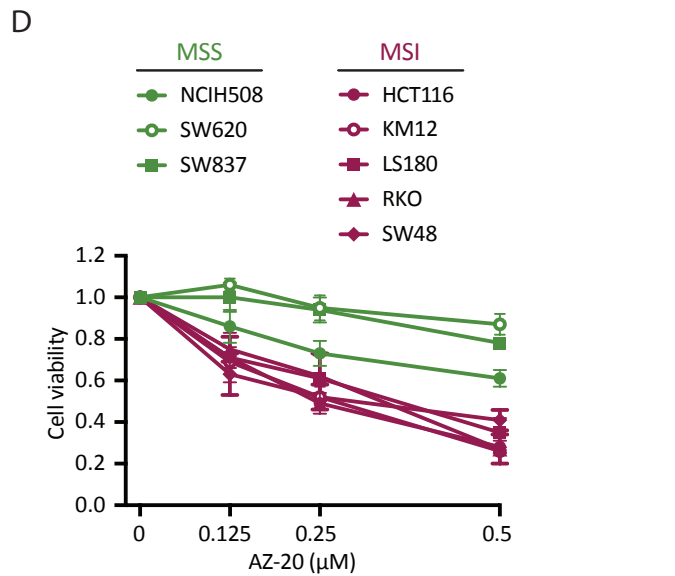
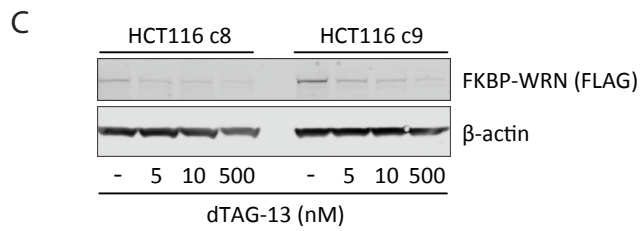
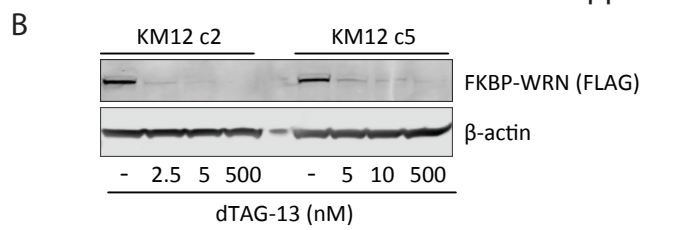
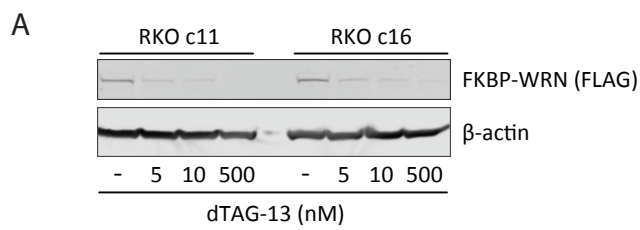
C



D

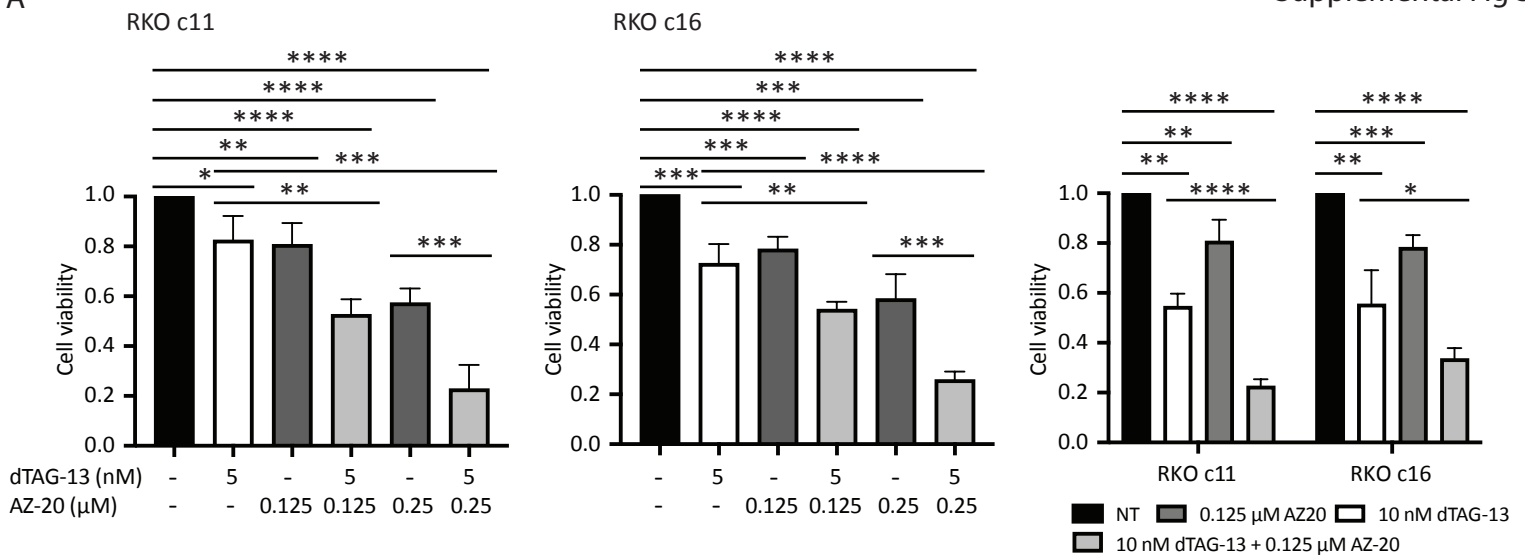


**Supplemental Figure S5. Lack of evidence for *bona fide* WRN resistance genes.** (A) RKO c17/Cas9 cells were transduced with individual sgRNAs targeting candidate WRN resistance genes identified from the CRISPR screen or a control sgRNA (ROSA) and subjected to growth competition assay (see Fig. 5D). Aliquots of vehicle- and dTAG-treated cells were taken after 24 h and the knockdown efficiency of target genes were determined by qRT-PCR. (B) Similar to (A), except that aliquots of vehicle- and dTAG-treated cells transduced with individual sgRNAs targeting candidate WRN resistance genes were processed for immunoblotting. Note that cells depleted for ILF3 were no longer able to efficiently degrade FKBP-WRN in response to dTAG-13. (C) A different clone of RKO (c16/Cas9) was transduced with individual sgRNAs targeting a subset of candidate WRN resistance genes and subjected to growth competition assays. (D) A clone of KM12 (c5/Cas9) was transduced with individual sgRNAs targeting a subset of candidate WRN resistance genes and subjected to growth competition assays. Note that only depletion of CRBN reproducibly rescued lethality in both dTAG-treated RKO and KM12 clones. A representative experiment is shown for each figure panel.

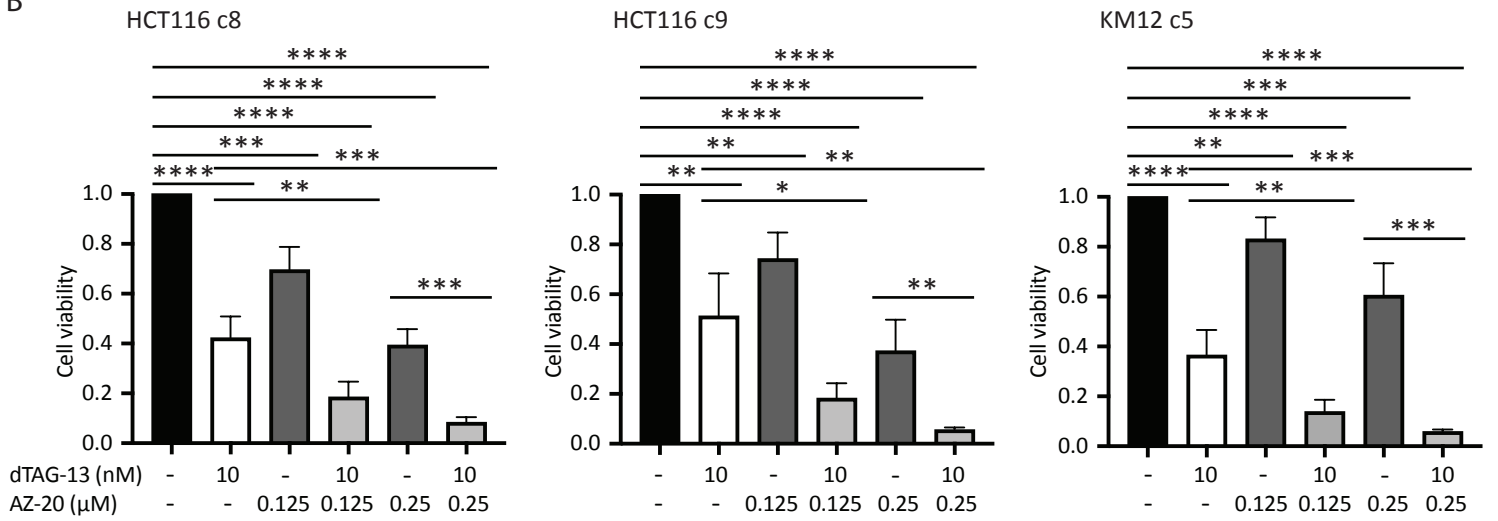


**Supplemental Figure S6. Dose-dependent cytotoxicity imparted by dTAG-13 and AZ-20 in human MSI-H cancer cells.** (A-C) RKO (A), KM12 (B) and HCT116 (C) clones expressing FKBP-WRN were treated or not with indicated doses of dTAG-13. After 24 h, cells were collected for immunoblotting (upper panels). A representative blot is shown. Cell viability was measured after 6 days (lower panels). Average (+/- S.D.) of six independent experiments is shown. (D) A larger panel of human MSI-H and MSS colorectal cancer cell lines were treated or not with indicated doses of AZ-20. Cell viability was measured after 6 days. Average (+/- S.D.) of three (RKO, KM12, LS180, SW48, NCIH508, SW620, SW837) to five (HCT116) independent experiments is shown. (E) MSI-H (RKO, KM12, HCT116 and MSS (NCIH508, SW837) cancer cells were treated or not with 0.5  $\mu$ M AZ-20 for 24 h (+ colcemid for the last 6 h). Analysis of metaphase spreads showed that ATR inhibition induced high levels of chromosomal aberrations in MSI-H but not MSS cells. Average (+/- S.D.) of three independent experiments. (F) The impact of WRN and ATR depletion on the fitness of human MSI-H vs MSS cancer cells (colorectal + endometrial). Publicly available data was downloaded from DepMap and re-plotted. (G) The cytotoxicity profiles of three ATR inhibitors in human MSI-H vs MSS cancer cells (colorectal + endometrial). A.U.C. values were downloaded from Genomics of Drug Sensitivity in Cancer (GDSC) or DepMap (PRISM repurposing screens) and re-plotted.

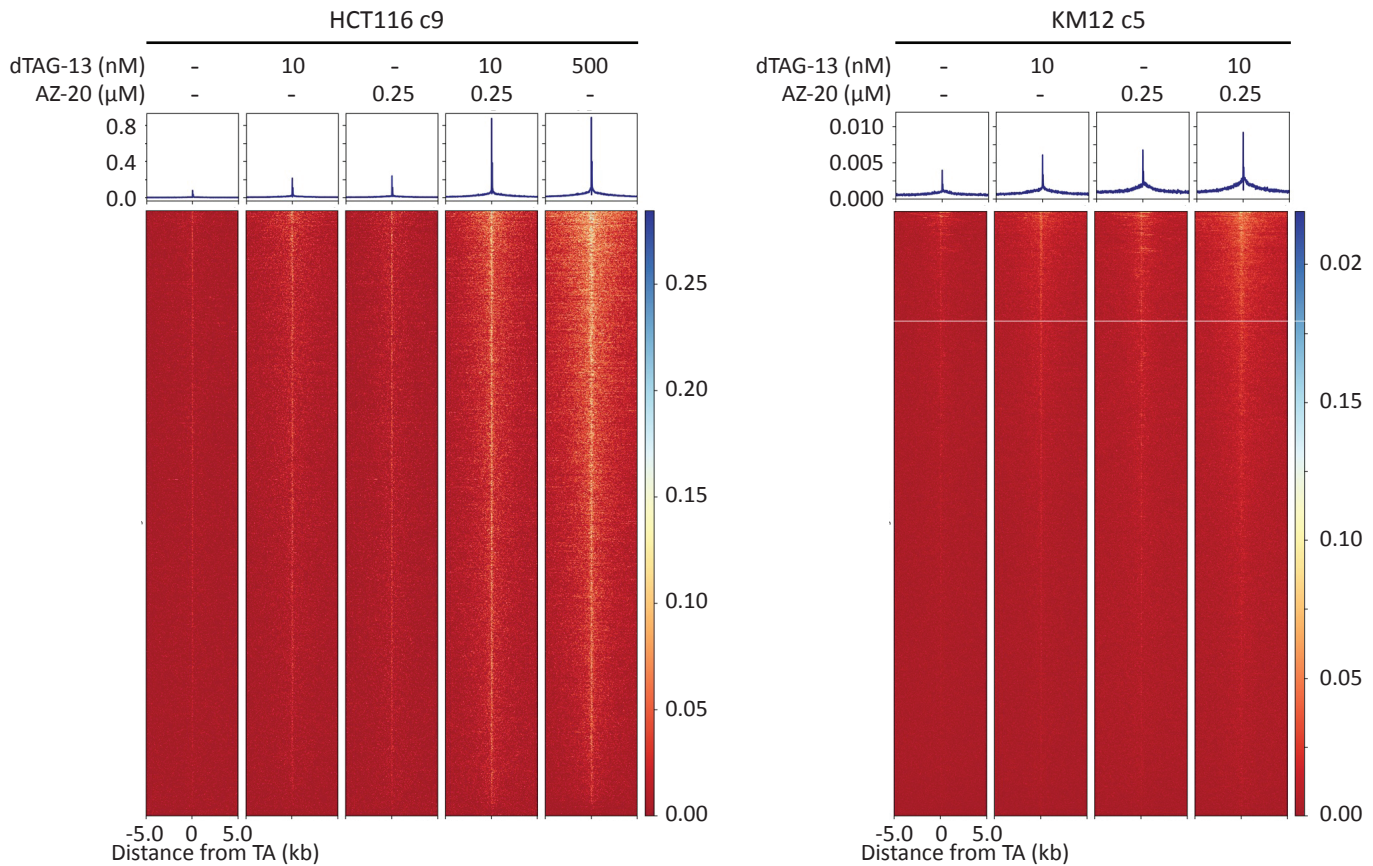
A



B



C



**Supplemental Figure S7. ATR co-inhibition enhances the cytotoxicity of low dose dTAG-13 treatment.** (A) RKO clones expressing FKBP-WRN were treated or not with the indicated doses of dTAG-13, AZ-20 or their combination. Average (+/- S.D.) of four independent experiments is shown. Cell viability was measured after 6 days. (B) Similar to (A) but in HCT116 and KM12 clones. Average (+/- S.D.) of four independent experiments is shown. (C) HCT116 (left panel) and KM12 (right panel) clones expressing FKBP-WRN were treated or not with the indicated doses of dTAG-13, AZ-20 or their combination for 24 h. END-seq showed that the combination regimen resulted in elevated levels of genomic breakage at expanded TA repeat regions, as compared to each single agent treatment.

**Supplemental Movie S1. Examples of dTAG-induced cell death events.** RKO reporter cells were treated 0.5  $\mu$ M dTAG-13 for and tracked by time-lapse microscopy. The events shown in this movie occurred between frames 270-310, which corresponded to 54-62 h after drug treatment. Note that during death, the nucleus could violently disintegrate or remain relatively intact.